ELSEVIER

Bioorganic & Medicinal Chemistry Letters

Bioorganic & Medicinal Chemistry Letters Vol. 16, No. 17, 2006

Contents

ARTICLES

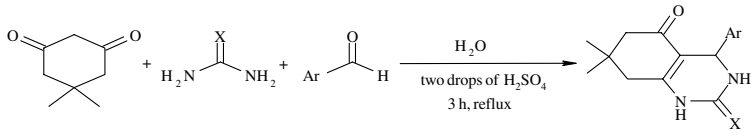

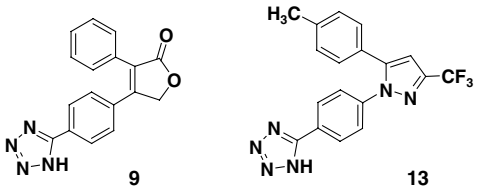

Design, synthesis, and evaluation of a new water-soluble, parenteral COX-2 inhibitor, rofecoxib (**9**) and celecoxib (**13**) analogues, in which the respective SO_2Me and SO_2NH_2 hydrogen-bonding pharmacophores were replaced by a tetrazole ring, are described.

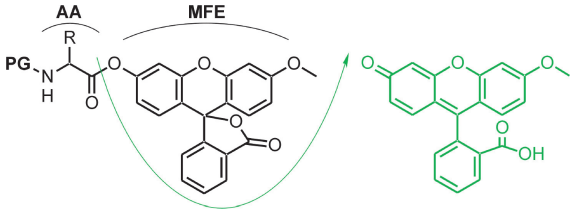

The synthesis of a new type of fluorogenic ester substrates is described. Prepared from fluorescein in three steps with common commercially available precursors, they generate bright green fluorescence upon proteolysis.

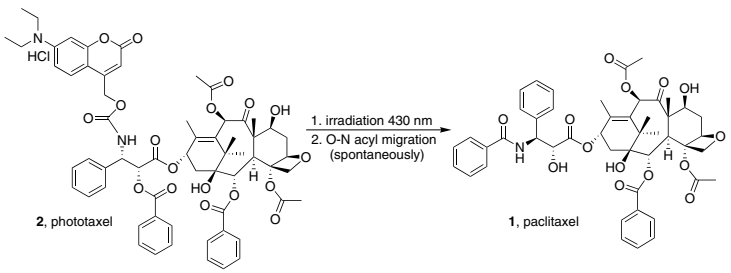

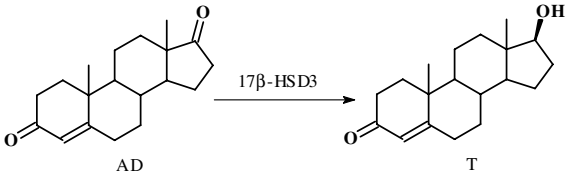

We report the preliminary results of the synthesis and biochemical evaluation of a number of novel inhibitors of type 3 isozyme of the enzyme 17β-hydroxysteroid dehydrogenase (17β-HSD3).

We describe the design and synthesis of dual-acting agents having both free radical scavenging and antithrombolic activities. These compounds may potentially be beneficial in treating myocardial ischemic/reperfusion injuries.

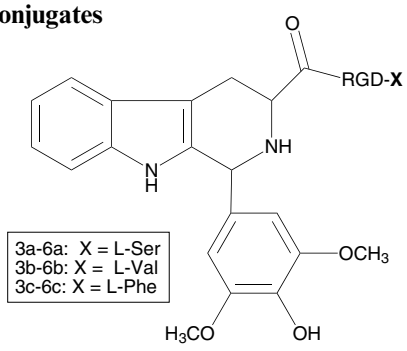

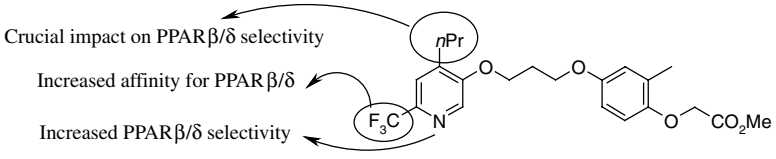

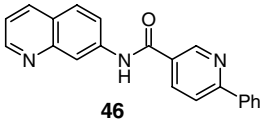

46

Starting from the high throughput screening hit (**3**), novel *N*-tetrahydroquinolinyl, *N*-quinolinyl and *N*-isoquinolinyl carboxamides have been identified as potent antagonists of the ion channel TRPV1. The *N*-quinolinylnicotinamide (**46**) showed excellent potency at human, guinea pig and rat TRPV1, a favourable *in vitro* DMPK profile and activity in an *in vivo* model of inflammatory pain.

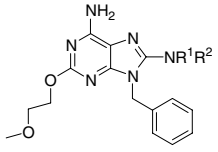

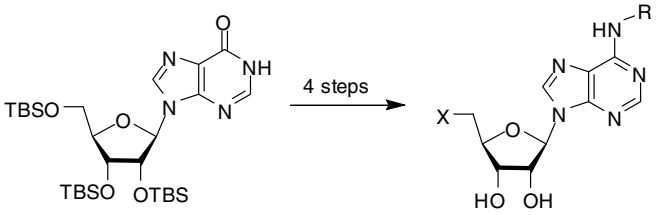

Adenosine analogues which are substituted at N^6 and/or modified at the 5′-position have been the subject of widespread interest. Herein we report a short and efficient synthesis of N^6-substituted 5′-modified adenosines, which was achieved in four steps from 2′,3′,5′-tris-*O*-(*tert*-butyldimethylsilyl)inosine.

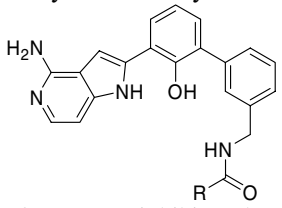

In our continued effort to develop orally bioavailable factor VIIa inhibitors based on the 2-[5-(5-carbamimidoyl-1*H*-benzoimidazol-2-yl)-6-hydroxy-biphenyl-3-yl]- succinic acid scaffold, we have identified potent and selective analogs with 4-amino-5-azaindole (1*H*-pyrrolo[3,2-*c*]pyridin-4-ylamine) as a less basic amidine replacement.

In the present investigation, 2-(4-formyl-2-methoxyphenoxy) acetic acid on condensation with various ketones in methanolic KOH solution yielded the corresponding chalcones (**1**–**3**). These corresponding chalcones were reacted with appropriate acid hydrazide in glacial acetic acid leading to the formation of phenoxy acetic acid derivatives. All newly synthesized compounds were evaluated for their anti-mycobacterial activities against *Mycobacterium tuberculosis* $H_{37}Rv$.

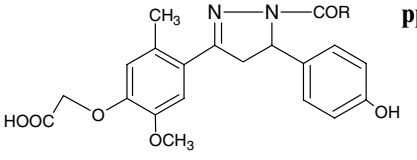

4-10

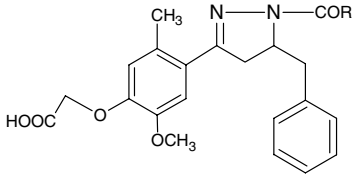

11-17

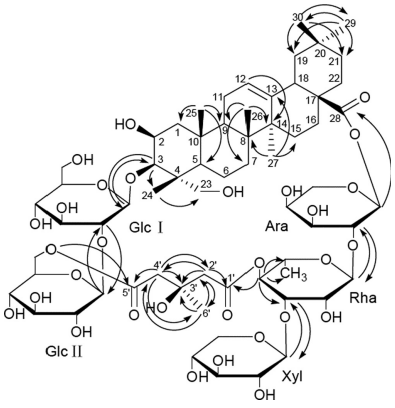

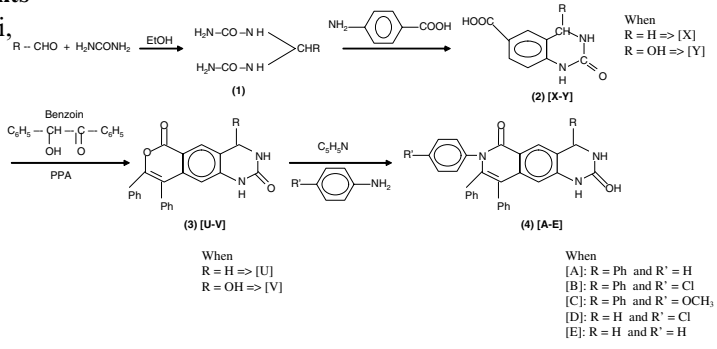

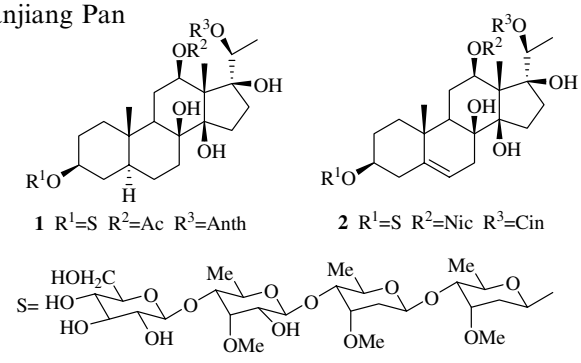

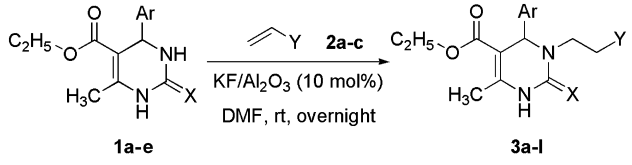

A simple and efficient method for the synthesis of *N3*-substituted 3,4-dihydropyrimidinones by aza-Michael addition reactions of 3,4-dihydropyrimidinones to α,β-ethylenic compounds catalyzed by KF/Al_2O_3 is described.

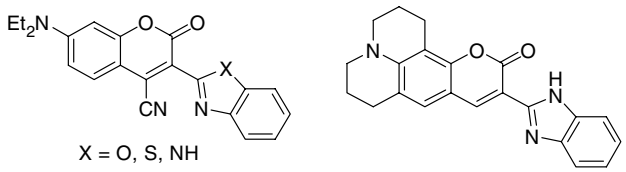

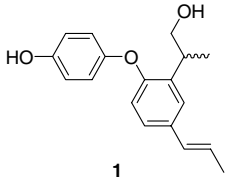

1

At a concentration of ca. 2 and 3μM, rodgersinol (**1**) inhibited 50% of the protein expression of iNOS and COX-2, respectively.

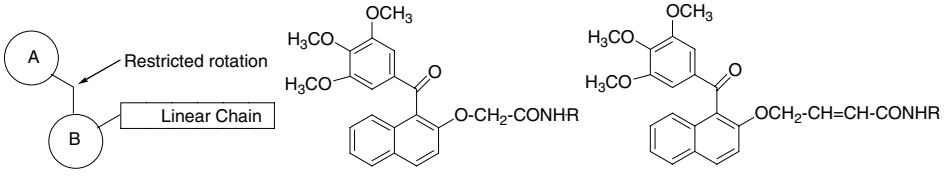

I II

Gallic acid has been modified to naphthophenone fatty acid amide derivatives. The targeted amides had a conformationally restricted pharmacophore and a linear aliphatic chain based on structure and activity relationship of previous studies. Two of the derivatives have shown significant cathepsin D inhibition activity having IC_{50} values 0. 056 and 0. 136μM.

A cyclic octapeptide, cyclosquamosin B (**2**), isolated from the seeds of *Annona squamosa* showed a vasorelaxant effect on rat aorta. It showed a slow relaxation activity against norepinephrine-induced contractions of rat aorta with/without endothelium. It showed inhibition effect on vasoconstraction of depolarized aorta with high concentration potassium, but moderate inhibition effect on NE-induced contraction in the presence of nicardipine.

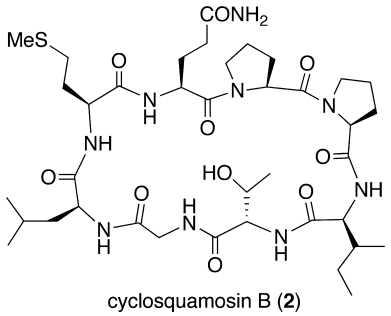

cyclosquamosin B (**2**)

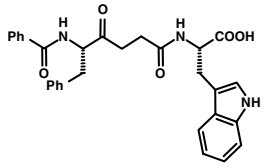

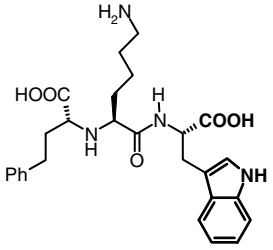

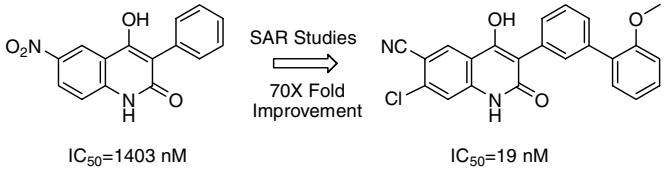

Oral administration of alcoholic extract of *Schouwia thebica* Webb showed that extracts are safe for human use, since it failed to induce death of mice in doses up to 4000 mg/kg body weight Hepatoprotective activity of the total alcoholic, diethyl ether, chloroform, ethyl acetate and *n*-butanol extracts were tested. It was found that the ethyl acetate and *n*-butanol extracts showed hepatoprotective activity. These extracts significantly reduced the increase in activities of ALT, AST, GGT, levels of glucose, triglycerides and cholesterol in serum of CCl_4 treated rats. The extracts showing hepatoprotective activity were found to contain a new flavonoid chrysoeriol-7-O-β-D-xylopyranoside-(1-2)-arabinofuranoside which was mainly found to be responsible for this activity when tested on lab animals alongside four flavonoids, known as chrysoeriol, Quercetin, quercetin-7-O-rhamnoside and kaempferol-3-O-β-D-glucoside. The structures were established by different spectroscopic techniques.

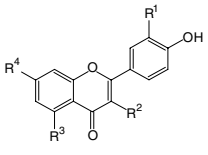

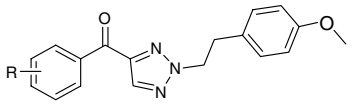

A series of novel (2-phenethyl-2*H*-1,2,3-triazol-4-yl)(phenyl)methanones were prepared and examined for utility as Kv1. 5 channel blockers for the treatment of atrial fibrillation.

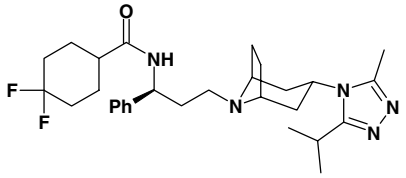

The discovery of maraviroc **17** is described with particular reference to the generation of high selectivity over affinity for the HERG potassium channel. This was achieved through the use of a high throughput binding assay for the HERG channel that is known to show an excellent correlation with functional effects.

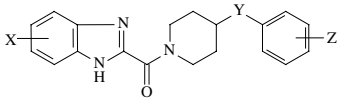

A novel series of benzimidazole-2-carboxamide derivatives was prepared and identified as NR2B selective NMDA receptor antagonists. The influence of some structural elements, like H-bond donor groups placed on the benzimidazole skeleton and the substitution pattern of the piperidine ring, on the biological activity was studied. Compound **6a** showed excellent analgetic activity in the mouse formalin test following po administration.

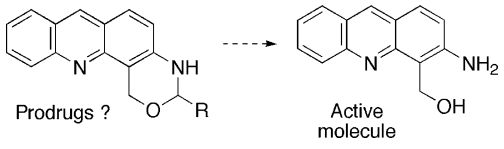

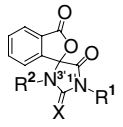

3d-p

The synthesis and anticonvulsant activity of the new phthalidyl spirohydantoins **3d–p** is reported, **3o** (R_1=C_2H_5, R_2=*p*-NO_2–C_6H_4, X = O) ED_{50} = 41. 8mg/kg.

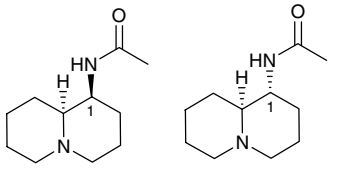

Epiquinamide *C(1)-Epi*epiquinamide

The synthesis of (±)-epiquinamide and (±)-*C*(1)-*epi*epiquinamide is reported. In a competition binding assay for [^{3}H]epibatidine binding to rat brain membranes neither ligand showed any significant level of nicotinic activity.

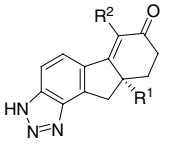

Several tetrahydrofluorenones with a triazole fused across C7–C8 showed high levels of ERβ-selectivity and were found to be potent ERβ-agonists. As a class they demonstrate improved oral bioavailability in the rat over a parent class of 7-hydroxy-tetrahydrofluorenones. The most selective agonist displayed 5. 7nM affinity and 333-fold selectivity for ERβ.

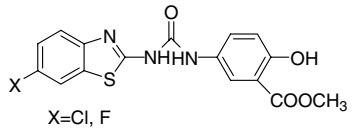

X=Cl, F

Small molecules that can prevent Aβ binding to the protein ABAD, a novel strategy for the treatment of Alzheimer's disease, were identified by high-throughput screening and chemical synthesis.

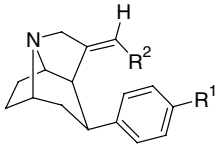

R^1 = -CH_3 Cl, Br,or I
R^2 = -H,or $COOCH_3$

A series of front bridged tricyclic 3β-(4′-halo or 4′-methyl)phenyltropanes bearing methylene or carbomethoxymethylene on the bridge to the 2β-position was synthesized, and their binding affinities to the human monoamine transporters were determined. All compounds studied in this series exhibit a moderate to high potency at all three transporters with SERT or DAT selectivity.

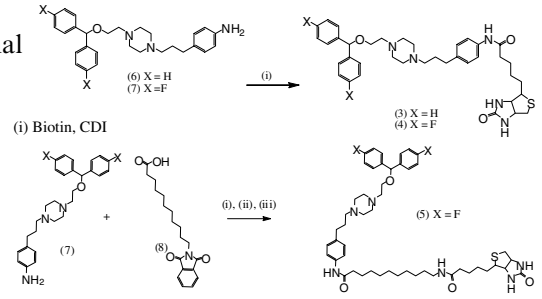

X = F, (i) Method A $SOCl_2$, CH_2Cl_2; Method B CDI; (ii) (a) Hydrazine, ethanol, (b) CH_2Cl_2; (iii) Biotin, NHS, DCC, DMF

The design and synthesis of a series of potent 1,3,4-trisubstituted-2-oxopiperazine based MC4 agonists are described. The tripeptidomimetics (**12a**,**b** and **23**) and the dipeptidomimetic **27** displayed single-nanomolar binding affinity and agonist potency for MC4R and excellent selectivity for MC4R relative to MC1R.

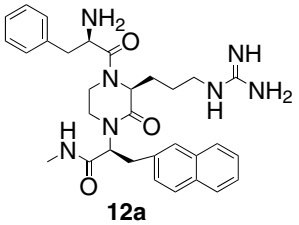

12a

	Ki, nM	EC50 (Emax, %), nM
MC4R	5.7	1.7 (105)
MC1R	659	526(108)

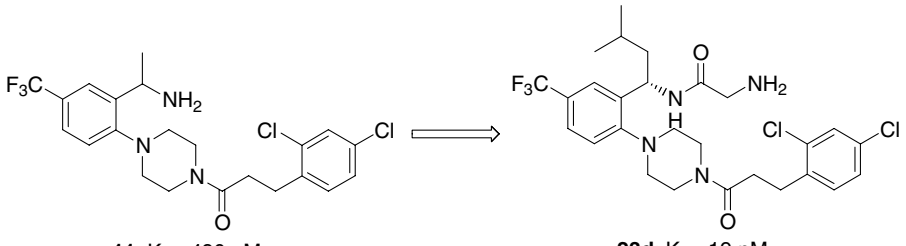

11: K_i = 490 nM

23d: K_i = 19 nM

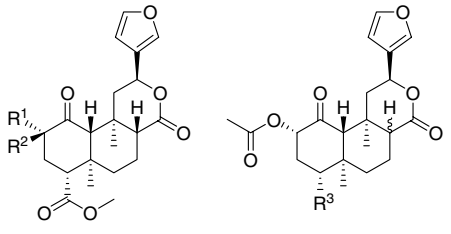

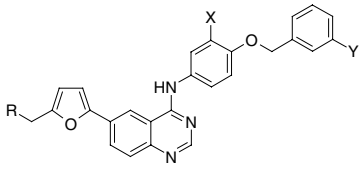

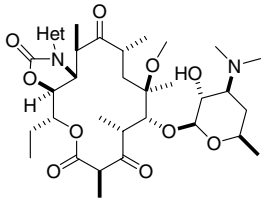

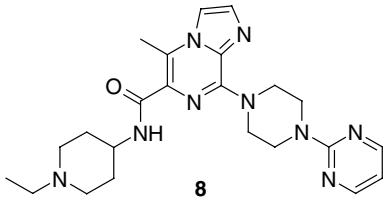

8

OTHER CONTENTS

*Corresponding author
ⓘ+ Supplementary data available via ScienceDirect

COVER

View of the crystal structure of the DB819-d(CGCGAATTCGCG)$_2$ complex, looking down the minor groove of the DNA (see Campbell, N.H.; Evans, D.A.; Lee, M.P.H.; Parkinson, G.N.; Neidle, S. *Bioorg. Med. Chem. Lett.* **2006**, *16*, 15). The DB819 molecule is shown in space-filling mode. Visualisation produced with the VMD program. [Humphrey, W.; Dalke, A.; Schulten, K. *J. Mol. Graphics* **1996**, *14*, 33.]

Indexed/Abstracted in: Beilstein, Biochemistry & Biophysics Citation Index, CANCERLIT, Chemical Abstracts, Chemistry Citation Index, Current Awareness in Biological Sciences/BIOBASE, Current Contents: Life Sciences, EMBASE/Excerpta Medica, MEDLINE, PASCAL, Research Alert, Science Citation Index, SciSearch, TOXFILE

ELSEVIER

ISSN 0960-894X